Influence of Geology and Hydrogeology on Heat Rejection from Residential Basements in Urban Areas

Author 1

Asal Bidarmaghz[✉], PhD

Lecturer in Geotechnical Engineering

School of Civil and Environmental Engineering, University of New South Wales, Sydney, Australia

Author 2

Ruchi Choudhary, PhD

Reader in Architectural Engineering

Department of Engineering, University of Cambridge, Trumpington Street CB2 1PZ, UK

Author 3

Kenichi Soga, PhD

Chancellor's Professor

Department of Civil and Environmental Engineering, University of California, Berkeley, USA

Author 4

Holger Kessler, MSc, FGS

British Geological Survey, Keyworth, Nottingham NG12 5GG, UK

Author 5

Ricky L. Terrington, MSc, CGeog (GIS)

British Geological Survey, Keyworth, Nottingham NG12 5GG, UK

Author 6

Stephen Thorpe, BSc

British Geological Survey, Keyworth, Nottingham NG12 5GG, UK

Full contact details of the corresponding author

Asal Bidarmaghz, Lecturer in Geotechnical Engineering

School of Civil and Environmental Engineering, University of New South Wales, Sydney, Australia

E-mail: a.bidarmaghz@unsw.edu.au

Abstract

Urbanization and limited land availability have resulted in the increased utilization of underground structures including residential basements in largely populated cities such as London, with an average addition of 200 basements per year in some boroughs. Residential basements kept at a comfortable temperature level throughout the year significantly contribute to heat fluxes in the subsurface as well as an increase in ground temperature. Understanding the ground thermal status is crucial in managing the significant geothermal energy potential in urban areas as well as the sustainable development of the urban underground, and in maintaining the energy efficiency of underground structures. In this proof-of-concept study, a 3D finite element approach accounting for coupled heat transfer and fluid flow in the ground was used to investigate the influence of ground conditions on the heat rejection rate from basements. A detailed analysis was made of ground, above ground and underground built environment characteristics. This study demonstrates that the amount of heat from basements rejected to the ground constitutes a significant percentage of the total heat loss from buildings, particularly in the presence of groundwater flow. The extent of thermal disturbance in the ground varies depending on the ground characteristics. The volume of ground thermal disturbance inversely correlates with the groundwater flow rate in the ground mainly consisting of granular (permeable) material. However, a direct correlation exists when the thickness of the granular layer decreases. A larger horizontal to vertical ratio of ground thermal disturbance is observed when the thickness of the permeable layer increases.

List of Notations

A_s	annual air swing [°C]
$C_{p,f}$	groundwater specific heat capacity [J/kgK]
$C_{p,m}$	solid material specific heat capacity [J/kgK]
$\mathbf{g}$	gravitational acceleration vector [m/s^2]
K	ground permeability [m^2]
k_h	ground hydraulic conductivity [m/s]
k_v	vegetation coefficient [-]
n	porosity [-]
p_f	pore pressure [Pa]
t	time of the year [day]
t_0	coldest temperature day from January 1st [day]
$T_{ground, mean}$	ground annual average temperature [°C]
T_m	temperature field in the ground [°C]
$\mathbf{v}_f$	groundwater velocity [m/s]
z	depth in the ground [m]
α	ground thermal diffusivity [m^2/s]
λ_{eff}	effective thermal conductivity of porous ground [W/mK]
λ_f	groundwater thermal conductivity [W/mK]
λ_m	solid material thermal conductivity [W/mK]
μ_f	groundwater dynamic viscosity [Pa.s]
ρ_f	groundwater density [kg/m^3]
ρ_m	solid material density [kg/m^3]

1. Introduction

Current rates of urbanization predict that 70% of the world's population will live in cities by 2050 (Un-Habitat, 2012). In addition to the above-ground landscape, underground built environments are an important feature of urbanization. In densely populated cities, where land is precious and planning laws constrain residential extensions above ground, underground spaces are attractive for different purposes, most commonly for transport and residential purposes. A review of recent planning applications for residential basements in London shows that basements which were used as cellars, storerooms and/or kitchens, are now mainly retrofitted to self-confined living flats or as an extension to the rest of the house providing additional living/leisure spaces[1][2][3][4]. These residential basements are likely to be kept at a comfortable temperature (18°C)[5] throughout the year. Given London's climate, where the annual average ground temperature is relatively low (12°C-14°C, (Price et al., 2018)) it is likely that residential basements continuously reject heat to the ground. A large increase in the number of heated basements in an urban area can thus result in a rise in temperature in the surrounding ground in the long term, especially in the presence of groundwater flow as it dissipates the heat away from the basements in the direction of groundwater flow affecting a greater area in the ground. The heat flux from a large number of basements into the ground accelerates the creation of an Urban Underground Heat Island (UUHI), where the ground is significantly warmer than its surroundings. The elevated ground temperature can be economically and environmentally advantageous in terms of geothermal energy exploitation. It is shown that the geothermal potential of urban areas is on average about 50% higher than in rural areas and can exceed the annual residential thermal demand in many urban areas (Arola and Korkka-Niemi, 2014, Zhu et al., 2010, Benz et al., 2015a, Menberg et al., 2013). Therefore, understanding the ground thermal disturbance in the urban underground is crucial to facilitate and manage geothermal energy exploitation in a sustainable manner.

UUHI and its impact on underground climate, in particular, groundwater flow network and temperature have been studied in varies cities (Attard et al., 2016a, Epting and Huggenberger, 2013, Menberg et al., 2013, Benz et al., 2015b, Attard et al., 2016b, Taniguchi et al., 2009, Ferguson and Woodbury, 2007, Ferguson and Woodbury, 2004). The heat flux into the subsurface as the heat input into shallow urban aquifers is caused by various anthropogenic heat sources. This includes increased ground surface temperature, solar radiation, buildings and basements, road tunnels, sewage networks, subway systems, reinjections of thermal wastewater and other geothermal energy systems such as ground source heat pumps (GSHPs). Buildings and basements are reported to have a significant impact on subsurface temperature with the maximum heat flux of between 10 W/m^2 and 16 W/m^2 (Menberg et al., 2013, Epting and Huggenberger, 2013).

Despite detailed studies on underground structures and heat rejection to the subsurface in various cities, the focus of most past research has been on identifying anthropogenic heat sources and quantifying the heat flux to the subsurface, as well as the consequent subsurface temperature increase via analytical and numerical approaches. Underground structures are significant contributors to subsurface temperature increase, and heat loss from these structures to the ground largely varies in different studies. However, to what extent ground conditions influence heat flux from underground structures to the subsurface has been mostly overlooked. This is due to the lack of detailed knowledge of the subsurface (e.g., limited ground temperature measurements, spatial heterogeneity of thermal conditions of the ground, the scale and complexity of the problem, etc.). The lack of reliable knowledge about urban underground has led to energy inefficiency in a number of structures. The high temperature in some underground train lines around the world and the passengers' thermal discomfort as a result represents one of the many problems which could have largely been prevented with a better understanding of the ground (Furfano et al., 2018, Ampofo et al., 2004, Cockram and Birnie, 1976). The aim of this paper is to investigate the extent to

---

[1] Arup 2008. Royal Borough of Kensington and Chelsea Town Planning Policy on Subterranean Development: Phase1-Scoping Study. London, UK.

[2] Baxter, A. 2013. Royal Borough of Kensington and Chelsea Residential Basement Study Report. London, UK.

[3] RBKC 2014. Basements Development Data: Partial Review of the Core Strategy. London, UK.

[4] RBKC 2009. Subterranean Development: Supplementary Planning Document. London, UK.

[5] Lane, M. 2011. How warm is your home. BBC Magazine. UK.

which thermally disturbed ground around heated basements is influenced by different geological and hydrogeological conditions. To what extent heat losses from basements and hence their thermal energy demand varies in different ground conditions is also investigated. The heat rejection rate from a set of heated residential basements in three districts with different geological and hydrogeological conditions was numerically modelled. In this study, we selected a representative London borough – The Royal Borough of Kensington and Chelsea (RBKC) – known for its high density of existing residential basements[6] (Baldwin et al., 2018). The LSOA[7] sub-divisions of RBKC were examined for their ground geology, number of residential basements, and hydrogeological properties. From these sub-divisions, three representative areas were selected for analysis and comparison. Each area has a similar number of basements, relatively similar surface area and similar hydraulic head differences. However, each has distinct combinations of geology types (varying between sand, gravel and clay), hence different hydraulic and thermal properties. The dominant building typology and the number of existing basements in RBKC were obtained from a detailed geo-mapping dataset[8]. The basement type and characteristics corresponding to the most dominant building type in the borough were corroborated through a comprehensive and time-consuming review of basement development applications submitted to RBKC planning and building control portal[9].

The geology and hydrogeology of the studied areas were extracted from a complex 3D geological model of RBKC aggregated at relevant resolutions. In this 3D model, the 2D ground hydro-thermal properties were spatially integrated into the model based on the geological classifications. Groundwater flow rate and direction play a key role in the temperature distribution of the ground. Therefore, groundwater level contours were extracted from the groundwater model developed for superficial deposits in RBKC accounting for the lost rivers (i.e., Fleet and Westbourne) as well as the River Thames (British Geological Survey, 2017).

2.   Above and underground characteristics of the Royal Borough of Kensington and Chelsea

2.1.1   Location and typology of basements

The Royal Borough of Kensington and Chelsea (RBKC) is known for large utilization of underground spaces, particularly as residential basements. High land price and construction constraints on above ground extensions have resulted in a significant appetite for underground expansion for residential purposes. Figure 1 shows that about 4,600 basement development proposals were made in seven boroughs in London between 2008-2017 (derived from the information provided by each borough's planning portal). About 1,022 approved basement development applications were extracted from RBKC's planning portal between these years (out of 1,300 basement development proposals made) demonstrating one of the highest basement development rates per household in the country (see Figure 1). These applications included around 676 standard basements (single storey, mostly under terraced houses), 279 large basements (double storey) and around 67 mega basements (triple storey or more- up to the depth of 18m), where basement developments are spread across the whole borough (Baldwin et al., 2018).

---

[6] D. Batty, C. Barr & P. Duncan, (2018). What lies beneath: the subterranean secrets of London's super-rich, The Guardian, UK.

[7] Lower Layer Super Output Areas (LSOAs) are a geographic hierarchy designed to improve the reporting of small area statistics in England and Wales and are generated to be as consistent in population size as possible. The Minimum population is 1000 and the mean is 1500.

[8] GeoInformation, (2017a). UK Buildings. Verisk Analytics.

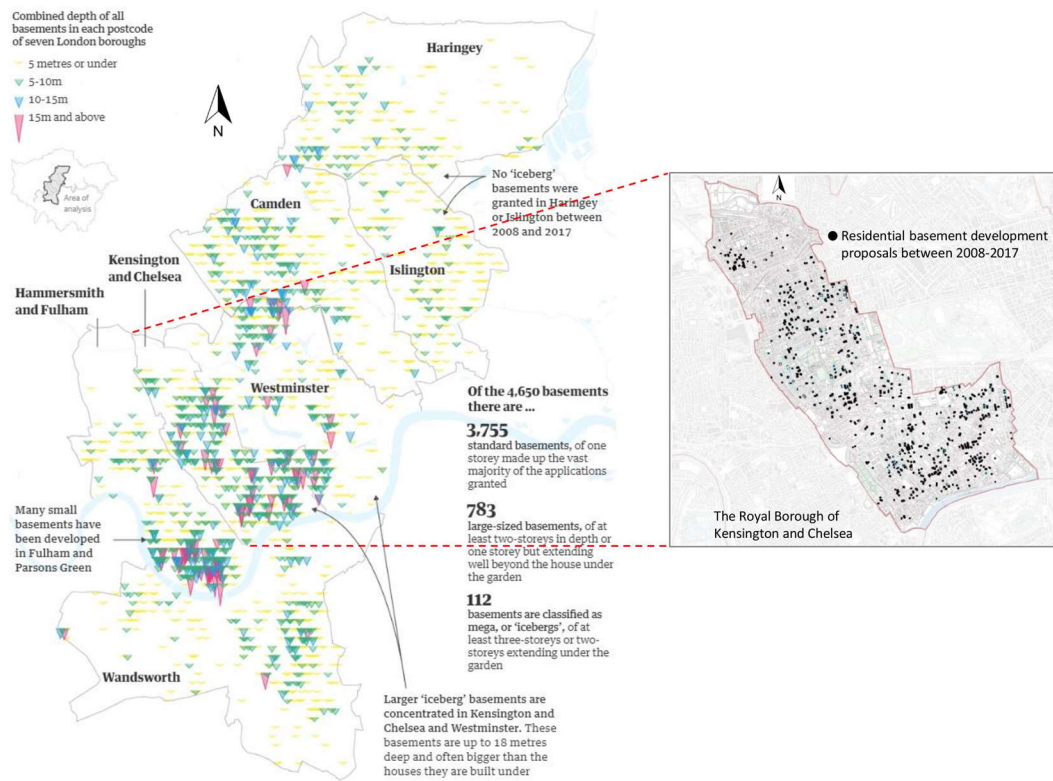[9] RBKC, (2018). Planning and Building Control Portal/Planning Search.

Figure 1. Basement proposals made in seven boroughs in London between 2008-2017 (Baldwin et al., 2018).

Reviewing the geo-mapping dataset confirmed the existence of 13,000 known residential basements in RBKC. Building typology, age, material and building height were some of the parameters analysed in this study to gain further insight into the characteristics of residential basements. About 22,000 residential buildings were identified

in RBKC, mainly varying between detached and semi-detached houses, flats and terrace houses (see

Figure 2).

Terrace houses are the most dominant building typology in this borough (i.e., 80%) owning 75% (10,000 out of 13,000) of the residential basements in RBKC. Knowing the most dominant building typology (terrace houses) in the borough and their corresponding building age, the characteristics of their basements were investigated by reviewing the basement development applications submitted to the planning and building control portal.

A comprehensive review of RBKC's planning and building control portal revealed that for most of the terrace houses, basements are single level and their floor area is similar to the building footprint. Even though RBKC possesses a large number of mega basements (around 200 according to (Baldwin et al., 2018)), these extra-deep basements ($\sim$18 m depth) were not the focus of this study as their overall impact on ground temperature on a district scale is negligible (in comparison to 13,000 standard, singe-level basements in the borough). In this study, the floor area per standard basement was assumed to be about 50 m^2, reflecting the basement of a typical two-bedroom terrace house and an average ceiling height of 3 m. A wall and slab thickness of 0.4 m, made of concrete, could be considered standard for these basements. The basements were assumed to be kept at a comfortable temperature level of 18°C throughout the year.

Figure 2. Residential building distributions in RBKC.

A 3D digital geological framework model of London, UK was developed by the British Geological Survey (BGS) (Burke et al., 2014, Mathers et al., 2014). The geological model was constructed at a scale equivalent to a 1:50 000 scale of 2D geological maps and comprises bedrock, superficial (Quaternary) deposits and artificial ground. It was constructed using GSI3D modelling software using the modelling procedures described by Kessler et al. (2009). Existing geological data derived from ground investigation boreholes were digitised using the method described by Burke et al. (2014).

The model developed by BGS for the area of RBKC was based on the 3D geolanduse layer that was a modified version of the 3D shrink-Swell clays dataset (Jones and Hulbert, 2017), which spans the surface to the top of the Chalk Group (shown in Figure 3-a). However, the geological layers extending from the surface to the top of the Lambeth Group was of interest to this work (60-100 below the ground surface). The 2D hydro-thermal datasets relevant to the geological classifications of the area were spatially integrated into the 3D model. Each grid cell of the model contains several characteristics of the ground such as geological units, ground elevation, groundwater level, hydro-thermal properties, etc. Figure 3-b shows the geological variations within the borough at different depths from the surface to 20 m depth (reaching the consistent London Clay Formation) using the 50 m x 50 m grids. Within the first 5 m below the surface, the southern part of the borough mostly consists of permeable River Terrace Deposits, whereas the northern part sits on impermeable London Clay Formation. However, it is observed that from about 10 m below the ground surface, the London Clay Formation dominates within the entire borough.
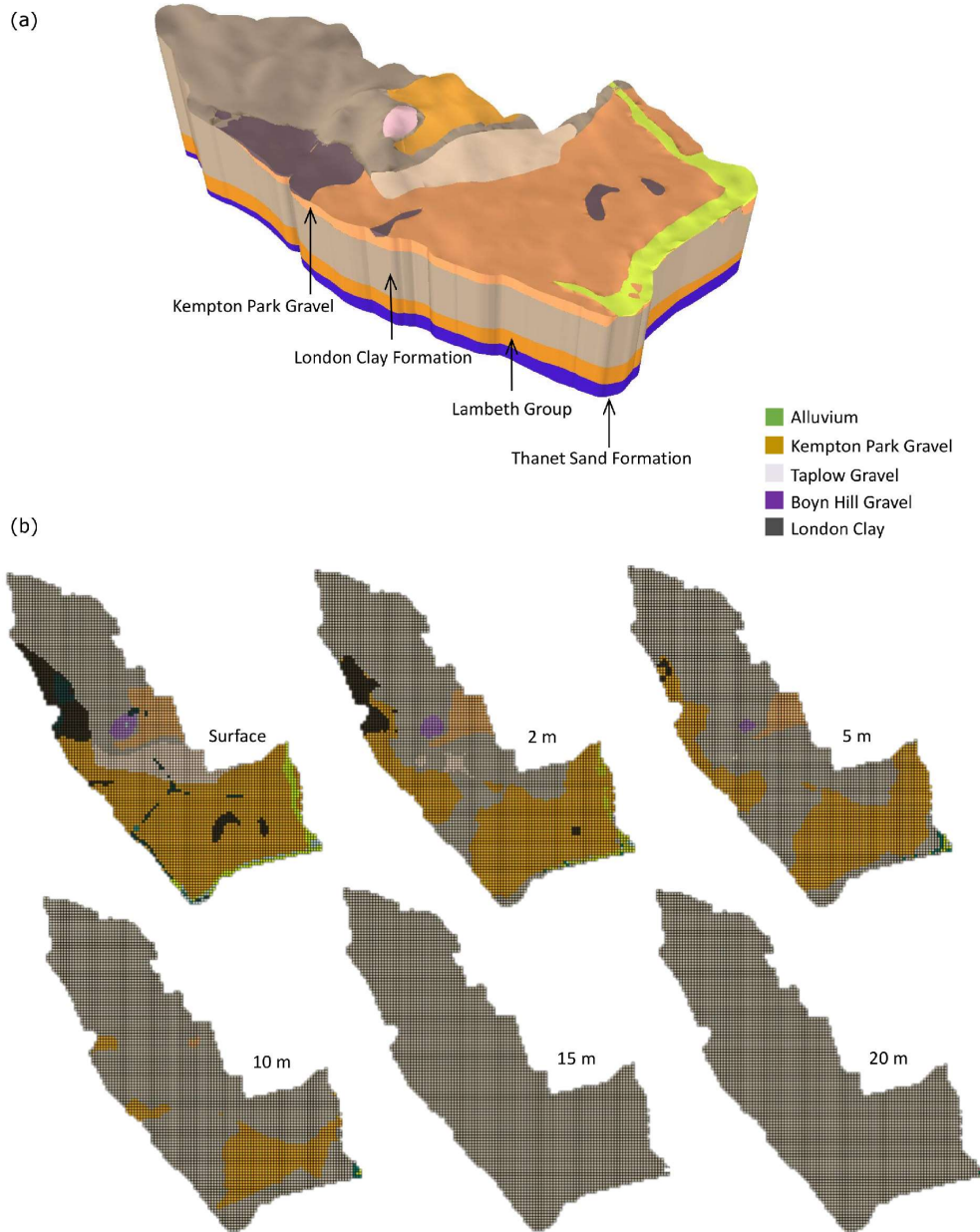
Figure 3. RBKC geology-50 m x 50 m grid (a): 3D geological model, (b): geological variations at different depths (not to scale).

The geology of RBKC is relatively consistent (the most significant variation occurs between the south and north part of the borough), therefore, LSOA subdivisions were used as cell grids in this study merging the attributes of 50 m x 50 m grids within each LSOA. By analysing the geological variations of each LSOA at different depths, one dominant geology was selected for each LSOA at a certain depth. Figure 4 shows a summary of the most dominant geological units for different areas of the borough varying by depth at the LSOA level, which shows a similar distribution within the borough as in the 50 m x 50 m grid model (Figure 3).
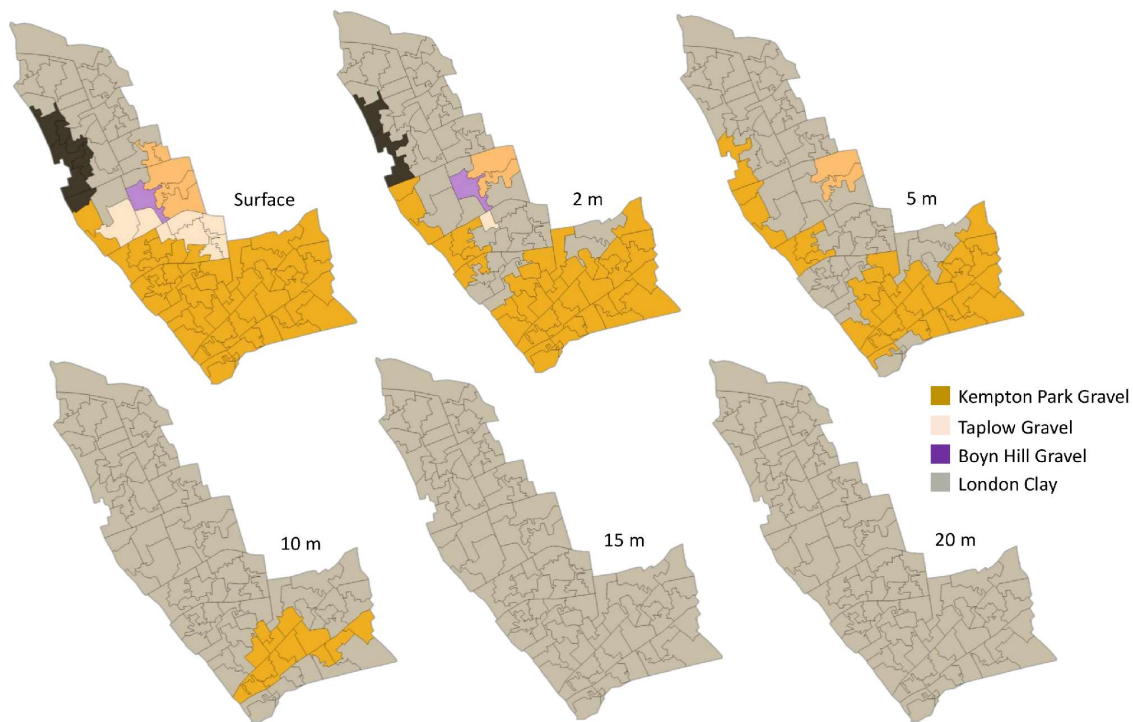
Figure 4. RBKC geological classification at LSOA level (not to scale).

According to Figure 4, geological classifications of LSOAs vary between four different geological units:

- 10 m of River Terrace Deposits underlain by London Clay Formation,
- 5 m of River Terrace Deposits underlain by London Clay Formation,
- 2 m of River Terrace Deposits underlain by London Clay Formation,
- London Clay Formation outcropping at the surface.

The River Terrace Deposits are deposits of sands and gravels, which can be up to 10 m thick. They are named differently and have slightly varying characteristics but can all generally be classified as sands and gravels (e.g., Kempton Park Gravel).

For the purpose of this study and according to different geological classifications identified in this borough, three groups each comprising LSOAs with similar geology (as shown in Figure 5) were selected as the geological representatives of the borough. Even though four variations of geology were identified in the borough, the area with 2 m of River Terrace Deposits underlain by London Clay Formation was not studied herein as it was expected to show similar results to the area where the London Clay Formation outcrops. The three areas selected possess similar ground volume and accommodate almost the same number of residential basements. This was essential to achieve a consistent $V_{basement}/V_{ground}$ (m^3) ratio in all areas and therefore a meaningful comparison within the areas.

Each area was studied independently and the thermal interaction between neighbouring areas was neglected in order to meet the objective of this paper, which was to examine the extent of ground temperature disturbance surrounding heated basements as well as the amount of heat loss variations from the basements to the ground in different ground conditions.
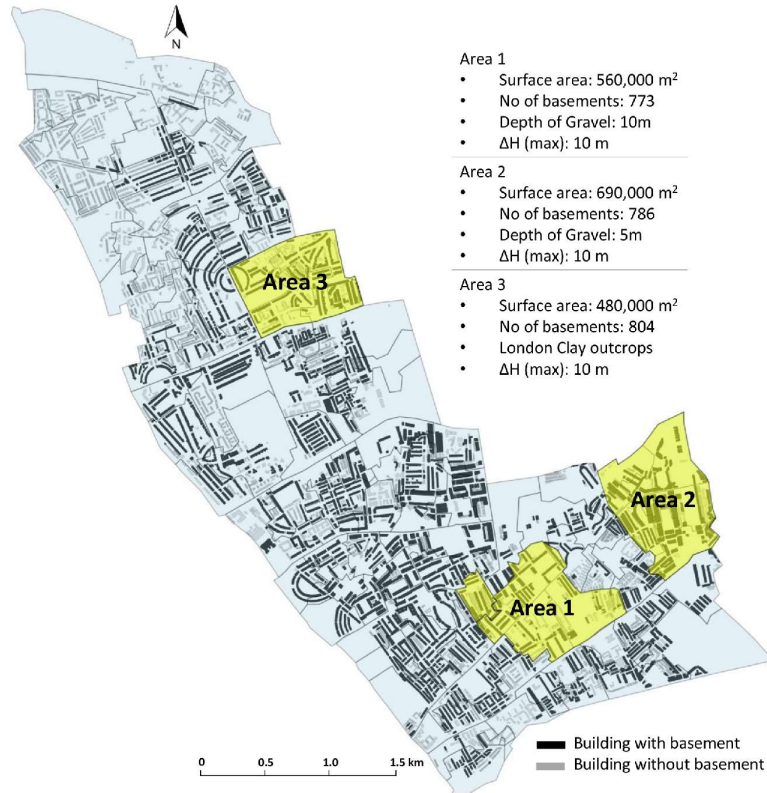
Area 1
• Surface area: 560,000 m²
• No of basements: 773
• Depth of Gravel: 10m
• ΔH (max): 10 m

Area 2
• Surface area: 690,000 m²
• No of basements: 786
• Depth of Gravel: 5m
• ΔH (max): 10 m

Area 3
• Surface area: 480,000 m²
• No of basements: 804
• London Clay outcrops
• ΔH (max): 10 m

Figure 5. Three different areas of Kensington and Chelsea selected for modelling.

2.1.2   Hydrogeology

The groundwater regime across the borough is generally characterised by two distinct aquifers which are separated by the relatively impermeable London Clay:

- the Upper Aquifer is perched water sitting in gravelly soils that overlie the London Clay;
- the Lower Aquifer within the sandy soils and chalk that lie deep below the London Clay.

For basements in the borough, the Upper Aquifer is most relevant. This is the water table that would be encountered when digging a basement.

The groundwater levels within the shallow aquifer can be extracted from the 3D geological model of RBKC. Considering the hydraulic conductivity of the superficial deposit and taking into account the lost rivers of Fleet and Westbourne and the River Thames (with an average recharge rate of 0.12 m/day- derived form BGS' Thames Basin recharge model), the resulting groundwater level contours are shown in Figure 6.

According to the groundwater contours, for the southern part of the borough (permeable superficial deposits) containing studied areas 1 and 2, a slight (around 0.25 m/day) groundwater flow can be identified. Even though the ground is relatively flat in the southern part of the borough, the water on this upper aquifer tends to flow slowly on the surface of the London Clay due to the high permeability of River Terrace Deposits. The northern part of the borough, containing area 3, mainly consists of impermeable London Clay Formation with negligible groundwater flow in that area.

This paper studied the effect of groundwater flow on ground temperature variations and the amount of heat loss from basements to the ground for different thicknesses of the permeable. Groundwater flow rate is a highly uncertain parameter, which plays a key role in ground temperature distribution. Therefore, to highlight the importance of groundwater flow rate on the thermal interaction between basements and the ground, several groundwater flow rate scenarios varying between 0 m/day (no flow), 0.5 m/day and 1 m/day were considered in this study. The extent to which thermally disturbed ground around a heated basement and the amount of heat loss

from basements to the ground are influenced by different hydrogeological conditions was numerically investigated in detail.
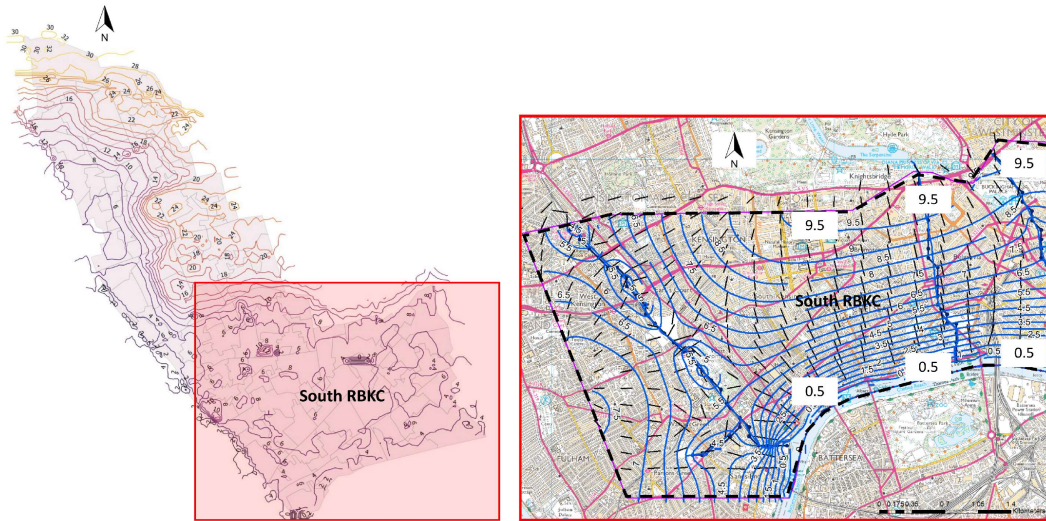

Figure 6. Groundwater level contours for the southern part of RBKC (British Geological Survey, 2017).

2.1.3   Ground hydro-thermal properties

Ground thermal properties are one of the most critical parameters for an accurate estimation of ground thermal disturbance due to their exposure to heat sources. Ground thermal conductivity and diffusivity used in this study were obtained from the 3D geological model for RBKC, where the general 2D thermal data classified for different geological units (mostly gathered from Thermal Response Tasting results around UK) are spatially integrated into the model (Price et al., 2018, Busby et al., 2009, British Geological Survey, 2017). The estimated values of thermal conductivity and diffusivity for Superficial Deposits and London Clay Formation are shown in Table 1.

In the presence of groundwater flow, ground hydraulic conductivity plays a significant role in the extent of heat propagation in the ground exposed to different sources of heat. In this study, the hydraulic conductivity of the superficial deposit was taken from a case study on the Thames Basin, UK. A conceptual model of superficial deposits across the Thames Basin was used to define different lithostratigraphic classes of superficial deposits including River Terrace Deposits. Hydraulic conductivity of the superficial deposits was estimated from grain-size distribution data, originally collected for mineral resource assessments, using the Kozeny–Carman method (Burke et al., 2014). The results are shown in Table 1. A relatively low hydraulic conductivity (1×10^{-9} m/s) was assumed for the impermeable London Clay.

Table 1. Estimated thermal/hydraulic conductivity and thermal diffusivity for some of the geological units in RBKC.

Geology		λ [W/(mK)]	α[m²/s]	k_h[m/s]
Kempton Park Gravel	0-2m depth	0.77	4.5×10^{-7}	4.2×10^{-5}
Kempton Park Gravel	2-10m depth	2.5	9.1×10^{-7}	5.6×10^{-4}
London Clay Formation	Various depths	1.79	9.7×10^{-7}	1×10^{-9}

3.   Thermal modelling of ground exposed to heated basements

Using a 3D finite element approach, the three selected areas of RBKC were modelled, accounting for the heated residential basements, ground surface cover, geological variations, and groundwater regime. The finite element package COMSOL Multiphysics was used to couple and solve the equations for conductive and convective heat transfer between the basements and the ground. The presented model is a representative of the selected areas in the borough. Each model (three models with the geometry presented in Figure 7) represents one of the three

selected areas (presented in Figure 5), each with a similar number of basements, similar ground surface area and similar geological and hydrogeological conditions to the real conditions.

3.1.1   Geometry and Meshing

Figure 7 shows the finite element representation of the ground exposed to heated basements and the initial and boundary conditions. Each area (model) accommodates about 800 basements in a volume of 1.5 km by 1.5 km by 90 m ground domain. To account for an even distribution of the basements in each area, four batches of 200 basements were considered in this study. The configuration of basement batches was selected randomly. The number of basements assumed in each model was taken from the approximate number of basements currently existing in the three areas shown in Figure 5**Error! Reference source not found.** These, and their floor areas, were derived from an extensive geospatial database containing footprint information per building and their use, age, and building type[10].

A depth of 3 m, including 0.4 m of slab thickness, and wall thickness of 0.4 m were considered for each basement. The floor area per basement was assumed to be 50 m^2, reflecting a typical two-bedroom terrace house. The whole model was meshed using triangular elements and was swept along the model resulting in about 600,000 elements.
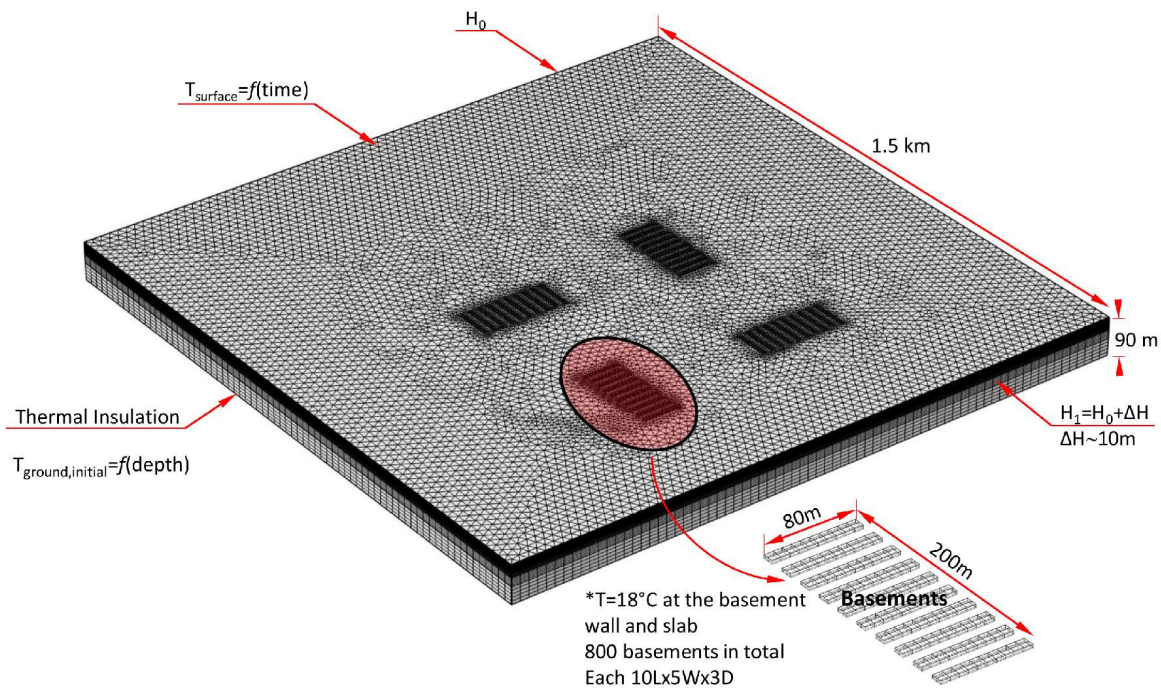

Figure 7. Schematic of 3D meshing and initial and boundary conditions.

3.1.2   Governing Equations

Heat transfer between the basements and the surrounding ground was captured by coupling and solving the equations for heat transfer and fluid flow in a porous medium (ground). The governing equations and initial and boundary conditions used in this study were previously validated in relation to a similar problem where heat transfer between the tunnel wall and the surrounding ground was investigated. Further details on validation of the coupling techniques and governing equations can be found elsewhere (Bidarmaghz, 2014, Bidarmaghz and Narsilio, 2018, Bidarmaghz et al., 2017, Makasis et al., 2018).

Heat conduction occurs in the ground and in the wall/floor of the basements. Unlike most of the literature considering a higher ground thermal conductivity (effective thermal conductivity) representing the groundwater,

---

[10] GeoInformation, (2017a). UK Buildings. Verisk Analytics.

the groundwater flow was numerically modelled in this study using Darcy's Law and heat convection occurring in the ground due to the presence of groundwater and its flow is modelled in detail. The conductive-convective heat transfer equations can be expressed as follows:

$$\left(\rho C_p\right)_{eff}\frac{\partial T_m}{\partial t} + \left(\rho C_p \boldsymbol{v_f}\right)\nabla T_m + \nabla.q = 0 \qquad 1$$

$$q = \lambda_{eff}\nabla T_m \qquad 2$$

$$\left(\rho C_p\right)_{eff} = (1-n)\rho_m C_{p,m} + n\rho_f C_{p,f} \qquad 3$$

$$\lambda_{eff} = (1-n)\lambda_m + n\lambda_f \qquad 4$$

where ρ_m represents the material density (i.e., ground, concrete, air), and $C_{p,m}$ and λ_m represent the specific heat capacity and thermal conductivity of the material respectively. Above, λ_f represents the thermal conductivity of the groundwater and λ_{eff} is the effective thermal conductivity of the porous ground. Note that other estimations may be used for λ_{eff} in Eq. 2; here we choose Eq. 4 for this. $C_{p,f}$ is the groundwater specific heat capacity, n is the porosity, and ρ_f is the groundwater density.

Single phase fluid flow in a porous medium (groundwater flow) is usually described by Darcy's law, which states that the Darcy velocity field, $\mathbf{v_f}$, is determined by the total head gradient $\nabla(pf - \rho_f gz)$, the fluid dynamic viscosity, μ_f, and the structure of the soil:

$$\boldsymbol{v_f} = -\frac{K}{\mu_f}\nabla\left(p_f - \rho_f gz\right) \qquad\qquad \frac{K}{\mu_f} = \frac{k_h}{\rho_f g} \qquad 5$$

where K is the isotropic permeability of the ground, p_f represents the pore pressure in the ground, ρ_f is the groundwater density, k_h is the hydraulic conductivity of the ground, $\mathbf{g}$ is the gravitational acceleration vector, and μ_f is the groundwater dynamic viscosity.

Inserting Darcy's Law into the continuity equations produces the generalized governing equation:

$$\frac{\partial}{\partial t}(n\rho) + \nabla.\rho\left[-\frac{K}{\mu_f}\nabla\left(p_f - \rho_f gz\right)\right] = 0 \qquad 6$$

Eqs. 5 and 6 are solved for $\mathbf{v}_f$ and p_f in the ground and are coupled to Eq. 1 via $\mathbf{v}_f$.

3.1.3 Initial & Boundary Conditions

To solve the above system of equations, appropriate initial and boundary conditions are required as shown in Figure 7 and are summarized as follows:

- The groundwater velocity of 0.25m/day is assigned to the model by introducing a hydraulic head gradient to the ground farfield boundaries. This is taken from the available groundwater level contours reflecting the average hydraulic head difference in the southern part of the borough. To further study the effect of groundwater flow rate on heat transfer between the basements and the ground, flow rates of 0m/day (no flow), 0.5m/day and 1m/day are also considered[11] (Burke et al., 2014).
- The basements' wall and floor are kept at the average indoor temperature in the UK (18°C) throughout the year[12].
- Thermal insulation is assigned to the building footprint on the surface to represent the thermally insulated building floor.

---

[11] Arup 2008. Royal Borough of Kensington and Chelsea Town Planning Policy on Subterranean Development: Phase1-Scoping Study. London, UK.
[12] How warm is your home, BBC Magazine, UK

- The undisturbed ground temperature is set at 12.5°C based on the temperature monitoring experiment in Earls's Court, London (Price et al., 2018).
- The seasonal changes in ground temperature are modelled as a time and depth varying temperature. This temperature is applied as a depth varying initial temperature to the entire model including the farfield ground boundaries and as a time-varying temperature to the ground surface to account for surface temperature fluctuations (Baggs, 1983, Jensen-Page et al., 2018, Bidarmaghz et al., 2016):

$$T_{ground}(z,t) = T_{ground,mean} - (1.07. k_v. A_s \times \exp(-0.000031552. z. \alpha^{0.5}) \times \cos\left(\frac{2\pi}{365}\right). (t - t_0 + 0.018335. z. \alpha^{0.5})$$

7

where $T_{ground,mean}$ is the ground annual average temperature, (12.5°C). k_v is the vegetation coefficient set at 0.5 accounting for 50% vegetation cover for each area. A_s, 8.3°C, is the annual air swing temperature. t is the day of the year. z indicates the depth in the ground [m]. α is the ground diffusivity equal to an average value of 9.65×10^{-7} m²/s, calculated based on physical and thermal properties of the soil presented in Table 2. t_0 is the coldest temperature day from January 1st (British Geological Survey, 2017, Price et al., 2018).

- The ground farfield boundary is set as thermal insulation instead of a time-depth varying temperature. In reality, the ground at farfield is also thermally disturbed when considering basements or other heat sources in adjacent areas. However, such thermal interference was not the focus of this proof-of-concept study.

A summary of the geological, physical and hydrothermal characteristics of the ground for the three areas modelled are presented in Table 2 (Busby et al., 2009, Price et al., 2018, British Geological Survey, 2017).

Table 2. Geological, physical and hydrothermal properties of the three areas shown in Figure 5.

	Area 1						
	Geology	*λ [W/(mK)]*	*ρ [kg/m³]*	*C_p [J/(kgK)]*	*Porosity[-]*	*k_h[m/s]*	*α[m²/s]*
0-2m	Kempton Park Gravel	0.77	1,600	1,100	0.35	4.2×10^{-5}	4.5×10^{-7}
2-10m	Kempton Park Gravel	2.5	1,900	1,440	0.35	5.6×10^{-4}	9.1×10^{-7}
10-90m	London Clay	1.7	2,000	870	0.5	1×10^{-9}	9.7×10^{-7}
	Area 2						
	Geology	*λ [W/(mK)]*	*ρ [kg/m³]*	*C_p [J/(kgK)]*	*Porosity*	*k_h[m/s]*	*α[m²/s]*
0-2m	Kempton Park Gravel	0.77	1,600	1,100	0.35	4.2×10^{-5}	4.5×10^{-7}
2-5m	Kempton Park Gravel	2.5	1,900	1,440	0.35	5.6×10^{-4}	9.1×10^{-7}
5-90m	London Clay	1.7	2,000	870	0.5	1×10^{-9}	9.7×10^{-7}
	Area 3						
	Geology	*λ[W/(mK)]*	*ρ [kg/m³]*	*C_p [J/(kgK)]*	*Porosity*	*k_h[m/s]*	*α[m²/s]*
0-90m	London Clay	1.7	2,000	870	0.5	1×10^{-9}	9.7×10^{-7}

4. Results and Discussions

Figure 8 shows the heat loss (W) from the wall and slab of one basement (10L×5W×3D) to the ground and its comparison to the heat loss from the above-ground structure of the buildings (house of 50m² floor area and 125m² of the exposed wall (from The Building Regulations, 2016). Depending on the thickness of the permeable layer

and groundwater flow rate, the heat rejection rate from the basements to the ground may be significant and comparable to the amount of heat loss from the above-ground structure of a newly built building to the air. These results are within the range of heat fluxes reported in the work of Epting et al. (2013) and Menberg et al (2013), where basements are constructed in saturated ground (~10 W/m^2 on average) (Epting and Huggenberger, 2013, Menberg et al., 2013).

Groundwater flow rate has less influence on the amount of heat losses from the basements to the ground, when the ground mianly consists of permeable material (area 1). However, when the thickness of the permeable layer decreases (area 2), faster groundwater flow leads to larger heat loss from basements and can become a significant percentage of the total heat loss from a building.

Underground structures constructed in impermeable soil, for example, most of the London Tube line constructed within London Clay Formation, have a consistent heat rejection rate into the ground due to minimal to negligable groundwater flow. However, heat transfer between the underground structures and the ground becomes more complex when groundwater flow is present. Heat rejection from heated basements constructed in the shallow ground with groundwater flow (permeable sand and gravel) varies significantly based on the geological distribution, and thickness of the permeable layer as shown in Figure 8. Therefore, the thermal energy demand for basements also varies and it is necessary to gain a better understanding of the ground thermal status in order to develop an efficient energy system design for underground structures.
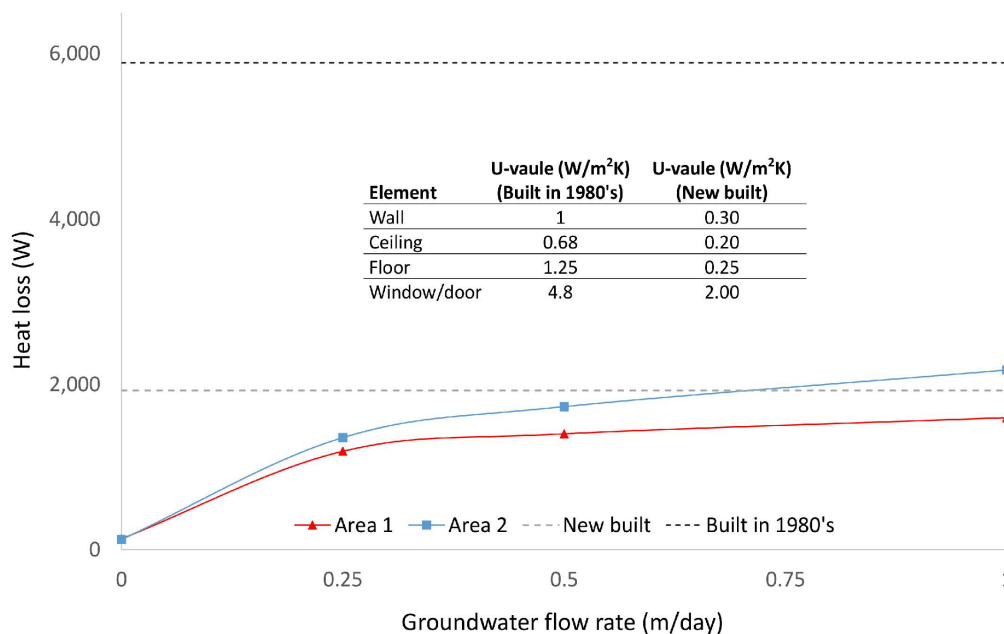

Element	U-vaule (W/m^{2}K) (Built in 1980's)	U-vaule (W/m^{2}K) (New built)
Wall	1	0.30
Ceiling	0.68	0.20
Floor	1.25	0.25
Window/door	4.8	2.00

Figure 8. Heat loss from basement wall and floor (one basement - 10L×5W×3D) for areas 1 and 2 and for typical double storey building (50 m^2 of floor area and 125 m^2 of the exposed wall) based on recommended U-values in 1980's and 2016[13].

Figure 9 shows the extent of the thermally affected ground with a temperature gradient of 1°C to 5.5°C with respect to the ground's annual average temperature (around 12.5°C) in vertical and horizontal directions in 25 years. For example, in area 1, the deepest point in the ground with a temperature gradient (T>12.5°C) occurs further away from the basement footprints in the direction of the groundwater flow and at the depth of 32m (Figure 9-a). The high permeability of the ground in area 1 affects the concentration of the thermal disturbance around the basements and leads to a faster heat dissipation to the farfield. However, in areas 2 and 3, the deepest point in the ground affected by the heated basements occurs at the depth of about 35m and 31m respectively (Figure 9-b

---

[13] The Building Regulations 2016. Conservation of Fuel and Power in New Dwellings. England.

and c). The combination of permeable layer thickness and groundwater flow rate in area 1 results in a larger horizontal extent of the disturbed ground (~400m from edge of basements) in comparison to area 2 (~250m) and area 3 (~10m) over 25 years. These results also show that the geothermal potential, its spatial concentration and extent also varies in the ground with different characteristics.
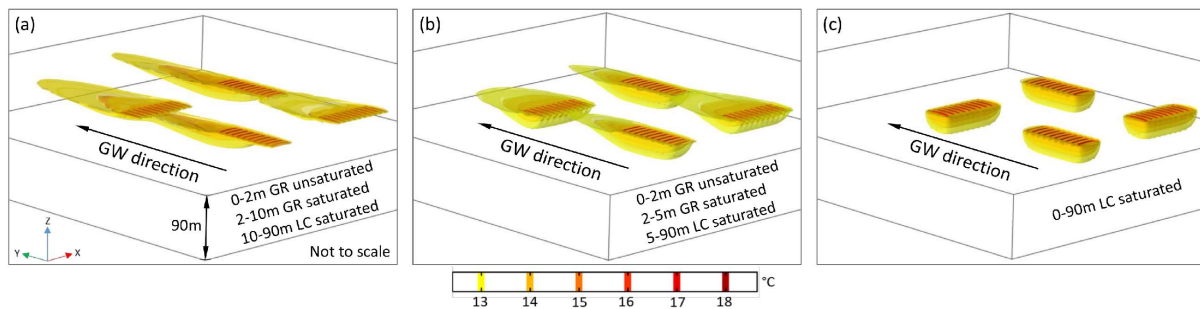

Figure 9. Thermally affected ground for 25 years with groundwater flow rate of 0.25m/day.

The modelled depth varying ground temperature profile - after 25 years of simulation - clearly shows the differences in ground temperature distributions for different areas (see Figure 10). The variations in ground temperature gradient (thermal discharge rate) are related to the permeable layer thickness. The highest temperature gradient (0.5°C/m) is observed for area 1 within the superficial deposit as shown in Figure 10. For area 2 where the permeable layer thickness is smaller, the temperature gradient is about 0.3°C/m for the first 5m (permeable layer). The temperature gradient is shown to be around 0.1°C for area 3, where the model consists of impermeable London Clay. It is also worth noting that depending on the thickness and thermal properties of the (superficial layer) permeable layer, the temperature gradient within the London Clay varies. This is due to the fact that the extent of thermal disturbance in the Clay is also dependent on the characteristics of the layer above. This is captured in the differences between temperature gradients in London Clay Formation for different models.

The limited ground temperature measurement in Earl's Court, London is shown in Figure 10 (triangular marks (Price et al., 2018)). The general temperature profile shows a similar trend to the temperature profile of modelled areas 2 and 3. The geological variation of the field is similar to area 3 with very thin Superficial Deposits, underlain by London Clay.
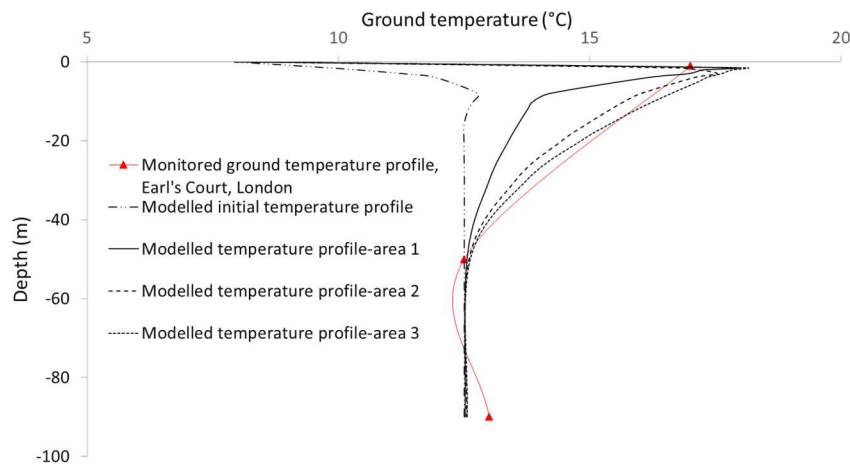

Figure 10. Measured and modelled temperature profiles.

Figure 11-a shows the volume of the ground with 1°C to 5.5°C temperature increase within 100m² of the basement footprint in 25 years. The volume of the thermally disturbed ground shows a non-consistent trend with an increase in groundwater flow rate. When the groundwater flow rate increases above 0.25m/day in area 1, the heat generated around the heated basements dissipates by fast flow. In area 2, on the other hand, the volume of the disturbed ground consistently increases for faster flows as the ease of heat transport in the ground is affected by the smaller volume of granular material leading to the accumulation of heat in the ground surrounding the basements. As

expected, the groundwater flow rate does not have a significant effect on area 3 due to the very low permeability of the clay material.

Figure 11-b shows the difference between area 2 and area 1 in terms of the maximum extent of the heated ground (with a temperature higher than the ground annual average temperature, 12.5°C) in the horizontal and vertical directions. In the horizontal direction, there is a significant difference with a relatively slow flow (0.25m/day) as area 1 extends 72% more in the horizontal direction than area 2. However, this difference decreases with an increase in groundwater flow rate, and at an extreme groundwater flow rate (1m/day) the difference is only about 3%. In ground with large volume of permeable layer (e.g., area 1), any two points at certain horizontal distances from the basements show a smaller temperature gradient than in area 2 where the thickness of the granular layer decreases. This is because the heat rejected from the basements is carried further away from the basement structure, resulting in a maximum temperature gradient (18°C-12.5°C=5.5°C) occurring at a larger length of the ground at any depth. However, in the case of an extreme groundwater flow rate, this effect is minimised. Therefore, areas 1 and 2 show a smaller difference in the horizontal extension of the thermally disturbed ground.

In the vertical direction, rejected heat from the basement is continuously dissipated in the direction of the groundwater flow in area 1 with largest volume of permeable material resulting in a shallower penetration depth of the heated area in the ground, which also decreases for faster groundwater flows (Figure 11-b).
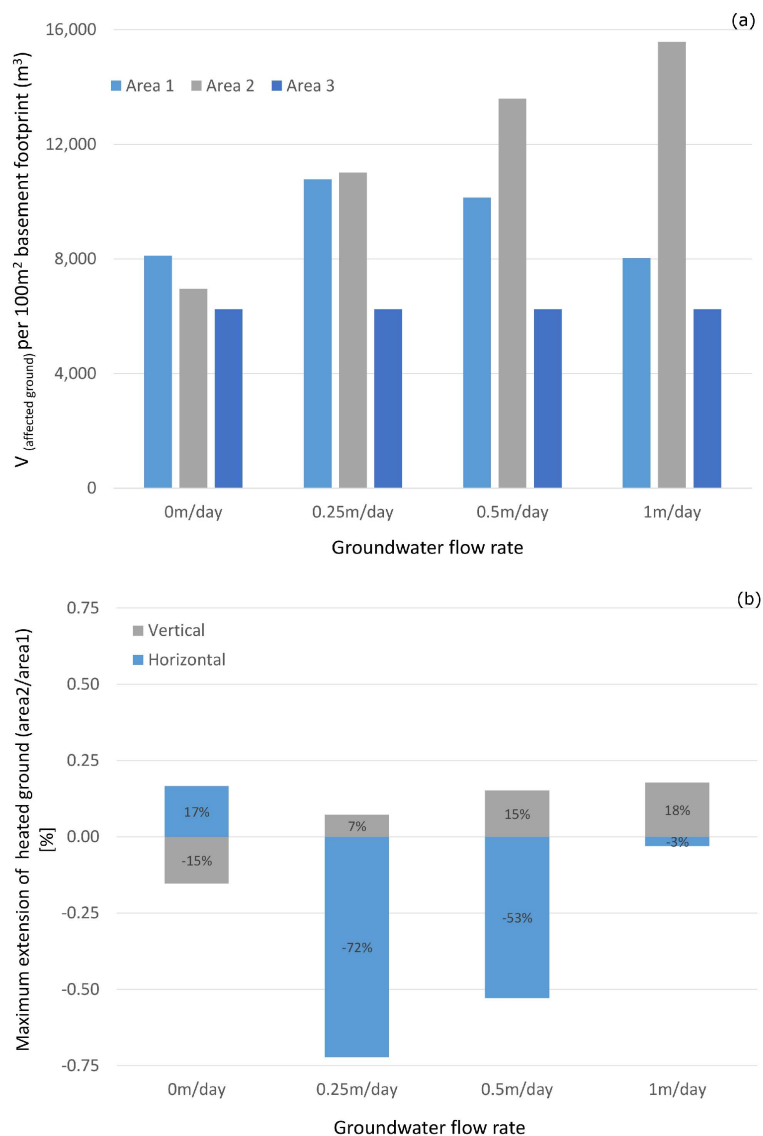
Figure 11. The thermally affected volume of the ground per 100m^2 of basement footprint (a), The difference between the extension of the heated ground in horizontal and vertical directions between the area 1 and area 2 (b).

5.   Conclusions

Reliable knowledge of ground thermal status in urban areas is crucial for 1) the sustainable development of underground structures, 2) the optimal utilization of geothermal sources and 3) efficient energy system design for underground structures. To achieve such understanding, not only are the built environment and external contributors (anthropogenic heat fluxes) to ground temperature rise important for consideration and study, but also analysis that is based on a good understanding of the local geological and hydrogeological conditions is required. The aim of this proof-of-concept study was to highlight the impact of geology and hydrogeology on the heat rejection rate from underground structures, and thus the extent of ground thermal disturbance. Numerical analysis of a sample of selected areas shows that thermal losses from heated basements to the ground can constitute a significant percentage of the total heat loss from a building, particularly in the presence of groundwater flow. However, this is not a consistent trend. Results show that the influence of groundwater flow on thermal loss from basements is less in ground with large volume of permeable material. In addition, the extent of thermal disturbance in the ground is also dependent on the combination of geological and hydrogeological characteristics. In ground mainly consisting of permeable material, the volume of the thermally affected ground shows an inverse correlation with the groundwater flow rate. It has a direct correlation with the groundwater flow rate in ground with the less permeable material. A larger horizontal to vertical ratio of thermal disturbance extension, which decreases in less permeable ground when ground is highly permeable.

The widely used assumption of constant annual average temperature for ground is demonstrated to be incorrect by this study. This incorrect assumption of the ground temperature has a direct impact on the evaluation of the energy requirements for basements. By using the ground as a source of geothermal energy, an accurate estimation of the ground temperature facilitates and improves the sustainable utilization of geothermal energy sources.

The understanding of the evolution of ground temperature necessitates a large-scale study on the thermal interaction between underground spaces and the surrounding ground. A city-scale model including different underground sources of heat (basements, train tunnels, etc.) is therefore required and will be the focus of our future work.

6.   Acknowledgement

7. References

Un-Habitat 2012. *State of the World's Cities 2008/9: Harmonious Cities*, Routledge.

Price, S. J., Terrington, R. L., Busby, J., Bricker, S. & Berry, T. 2018. 3D ground-use optimisation for sustainable urban development planning: A case-study from Earls Court, London, UK. *Tunnelling and Underground Space Technology,* 81**,** 144-164.

Arola, T. & Korkka-Niemi, K. 2014. The effect of urban heat islands on geothermal potential: examples from Quaternary aquifers in Finland. *Hydrogeology Journal,* 22**,** 1953-1967.

Zhu, K., Blum, P., Ferguson, G., Balke, K.-D. & Bayer, P. 2010. The geothermal potential of urban heat islands. *Environmental Research Letters,* 5**,** 044002.

Benz, S. A., Bayer, P., Goettsche, F. M., Olesen, F. S. & Blum, P. 2015a. Linking surface urban heat islands with groundwater temperatures. *Environmental science & technology,* 50**,** 70-78.

Menberg, K., Blum, P., Schaffitel, A. & Bayer, P. 2013. Long-term evolution of anthropogenic heat fluxes into a subsurface urban heat island. *Environmental science & technology,* 47**,** 9747-9755.

Attard, G., Winiarski, T., Rossier, Y. & Eisenlohr, L. 2016a. Impact of underground structures on the flow of urban groundwater. *Hydrogeology journal,* 24**,** 5-19.

Epting, J. & Huggenberger, P. 2013. Unraveling the heat island effect observed in urban groundwater bodies– Definition of a potential natural state. *Journal of hydrology,* 501**,** 193-204.

Benz, S. A., Bayer, P., Menberg, K., Jung, S. & Blum, P. 2015b. Spatial resolution of anthropogenic heat fluxes into urban aquifers. *Science of The Total Environment,* 524**,** 427-439.

Attard, G., Rossier, Y., Winiarski, T. & Eisenlohr, L. 2016b. Deterministic modeling of the impact of underground structures on urban groundwater temperature. *Science of The Total Environment,* 572**,** 986-994.

Taniguchi, M., Shimada, J., Fukuda, Y., Yamano, M., Onodera, S.-i., Kaneko, S. & Yoshikoshi, A. 2009. Anthropogenic effects on the subsurface thermal and groundwater environments in Osaka, Japan and Bangkok, Thailand. *Science of the total environment,* 407**,** 3153-3164.

Ferguson, G. & Woodbury, A. D. 2007. Urban heat island in the subsurface. *Geophysical research letters,* 34.

Ferguson, G. & Woodbury, A. D. 2004. Subsurface heat flow in an urban environment. *Journal of Geophysical Research: Solid Earth,* 109.

Furfano, D., Liebson, R. & Brown, R. 2018. Now subway platfrom temperature feels like hell, too. *New York Post.*

Ampofo, F., Maidment, G. & Missenden, J. 2004. Underground railway environment in the UK Part 2: Investigation of heat load. *Applied Thermal Engineering,* 24**,** 633-645.

Cockram, L. J. & Birnie, G. R. the ventilation of London underground railways. 2nd International Symposium on the Aerodynamics and Ventialtion of Vehicle Tunnels, 1976 Cambridge, England.

Baldwin, S., Holyord, E. & Burrows, R. 2018. Mapping the Subterranean Geographies of Plutocratic London: Luxified Troglodytism?

British Geological Survey. 2017. *RE: Ground Thermal and Hydraulic Property Data.*

Burke, H., Mathers, S., Williamson, J., Thorpe, S., Ford, J. & Terrington, R. 2014. The London Basin superficial and bedrock LithoFrame 50 Model.

Mathers, S., Burke, H., Terrington, R., Thorpe, S., Dearden, R., Williamson, J. & Ford, J. 2014. A geological model of London and the Thames Valley, southeast England. *Proceedings of the Geologists' Association,* 125**,** 373-382.

Kessler, H., Mathers, S. & Sobisch, H.-G. 2009. The capture and dissemination of integrated 3D geospatial knowledge at the British Geological Survey using GSI3D software and methodology. *Computers & geosciences,* 35**,** 1311-1321.

Jones, L. & Hulbert, A. 2017. User Guide for the Shrink-Swell 3D (GeoSure Extra) dataset V1.0. *In:* LEE, K. (ed.). Keyworth, Nottingham, UK: British Geological Survey.

Busby, J., Lewis, M., Reeves, H. & Lawley, R. 2009. Initial Geological Considerations Before Installing Ground Source Heat Pump Systems. *Quarterly Journal of Engineering Geology and Hydrogeology,* 42**,** 295-306.

Bidarmaghz, A. 2014. *3D numerical modelling of vertical ground heat exchangers.* PhD Thesis, The University of Melbourne.

Bidarmaghz, A. & Narsilio, G. 2018. Heat exchange mechanisms in energy tunnel systems. *Geomechanics for Energy and the Environment.*

Bidarmaghz, A., Narsilio, G. A., Buhmann, P., Moormann, C. & Westrich, B. 2017. Thermal Interaction Between Tunnel Ground Heat Exchangers and Borehole Heat Exchangers. *Geomechanics for Energy and the Environment,* 10**,** 29-41.

Makasis, N., Narsilio, G. A., Bidarmaghz, A. & Johnston, I. W. 2018. Ground-source heat pump systems: the effect of variable pipe separation in ground heat exchangers. *Computers and Geotechnics,* 100**,** 97-109.

Baggs, S. A. 1983. Remote prediction of ground temperature in Australian soils and mapping its distribution. *Solar Energy,* 30**,** 351-366.

Jensen-Page, L., Narsilio, G. A., Bidarmaghz, A. & Johnston, I. W. J. R. e. 2018. Investigation of the effect of seasonal variation in ground temperature on thermal response tests. 125**,** 609-619.

Bidarmaghz, A., Narsilio, G., Johnston, I. & Colls, S. 2016. The importance of surface air temperature fluctuations on long-term performance of vertical ground heat exchangers. *Geomechanics for Energy and the Environment,* 6**,** 35-44.